an analogous experiment by using a denaturant, guanidine hydrochloride, with the peptides EAK, ELK, and EGK at different temperatures. The two-state equilibrium constant for the helix-coil transition is $K_h = f/(1 - f)$.
22. S. P. Ho and W. F. DeGrado, *J. Am. Chem. Soc.* **109**, 6751 (1987).
23. P. S. Kim and R. L. Baldwin, *Nature* **307**, 329 (1984); J. W. Nelson and N. R. Kallenbach, *Biochemistry* **28**, 5256 (1989).
24. A summary of methods is given in K. Wüthrich, *NMR of Proteins and Nucleic Acids* (Wiley, New York, 1986), p. 166. Data on the EXK peptides are from M. I. Liff, P. C. Lyu, N. R. Kallenbach, *Polym. Prepr.* **31**, 139 (1990), and unpublished results.
25. D. G. Davis and A. Bax, *J. Am. Chem. Soc.* **107**, 2820 (1985).
26. A. Kumar, R. R. Ernst, K. Wüthrich, *Biochem. Biophys. Res. Commun.* **95**, 1 (1980).
27. L. Szilagyi and O. Jardetzky, *J. Magn. Reson.* **83**, 441 (1989).
28. This model is equivalent to expanding the Zimm-Bragg (*6*) partition function in the limit of single helical sequences in short chains, retaining terms that are linear in σ, taken to be 1×10^{-3} [based on experimental data on Lys polymers, T. V. Barskaya and O. B. Ptitsyn, *Biopolymers* **10**, 2181 (1971), as well as the mean value from theoretical calculations by A. Englert *et al.*, *Macromolecules* **8**, 655 (1975)]. With the additional factor that the CD signal for a helix varies with the number of helical residues [we use the approximation that for a helix of k residues, $[\theta(k)]_{222} = [\theta]_{100}(1 - 1/k)$], the value of $[\theta]_{222}$ for any given chain can be calculated if the appropriate s values are known or can be estimated. The limiting values of $[\theta]_{100}$ and $[\theta]_0$ determined as described in (*21*) are also used for this calculation.
29. L. Serrano and A. R. Fersht, *Nature* **342**, 296 (1989); Ser was introduced at position 2 in the EXK peptides to provide a positive N capping effect.
30. P. C. Lyu, P. Wang, M. I. Liff, N. R. Kallenbach, unpublished results.
31. Supported by NIH grants GM 40746 and RR 02497 and NSF grants DIR 8722895 and DMB 84-13986. We thank W. F. DeGrado for sharing data and for helpful discussions.

4 May 1990; accepted 4 September 1990

Increased Activity of Calcium Leak Channels in Myotubes of Duchenne Human and *mdx* Mouse Origin

PEYING FONG, PAUL R. TURNER, WILFRED F. DENETCLAW, RICHARD A. STEINHARDT*

Elevated free Ca^{2+} concentrations found in adult dystrophic muscle fibers result in enhanced protein degradation. Since the difference in concentrations may reflect differences in entry, Ca^{2+} leak channels in cultures of normal and Duchenne human myotubes, and normal and *mdx* murine myotubes, have been identified and characterized. The open probability of leak channels is markedly increased in dystrophic myotubes. Other channel properties, such as mean open times, single channel conductance, ion selectivity, and behavior in the presence of pharmacological agents, were similar among myotube types. Compared to the Ca^{2+} concentrations in normal human and normal mouse myotubes, intracellular resting free Ca^{2+} concentrations ($[Ca^{2+}]_i$) in myotubes of Duchenne and *mdx* origin were significantly higher at a time when dystrophin is first expressed in normal tissue. Taken together, these findings suggest that the increased open probability of Ca^{2+} leak channels contributes to the elevated free intracellular Ca^{2+} concentration in Duchenne human and *mdx* mouse myotubes.

ADULT *mdx* SINGLE SKELETAL FIBERS have higher levels of intracellular free Ca^{2+} than normal mouse skeletal fibers; these elevated Ca^{2+} concentrations correlate with increased protein degradation rates in the dystrophic condition (*1*). The defective gene responsible for Duchenne muscular dystrophy in humans and the dystrophic condition of the *mdx* mouse results in the absence of dystrophin in muscle cells and brain tissue (*2–4*). Dystrophin is localized primarily to the sarcolemma of skeletal muscle fibers (*5, 6*). The dystrophin NH_2-terminal coding sequence is similar to that of α-actinin and may be involved in the anchorage of F-actin filaments to cell membranes (*7, 8*). Dystrophin is associated with the cell membrane by attachment to an integral membrane protein (*9, 10*). We hypothesized that the basic mechanism underlying the pathology of muscular dystrophy could involve the modulation of Ca^{2+} leak channels whose properties are altered by the absence of dystrophin.

Higher concentrations of free $[Ca^{2+}]_i$ measured in freshly dissected intact skeletal muscle fibers from mice, as well as in 3-week-old cultured human myotubes, correlated with the absence of dystrophin (*1, 11*). Before we could test any hypothesis of how $[Ca^{2+}]_i$ becomes elevated in dystrophic tissues, it was necessary to establish that the defect in Ca^{2+} regulation was present in the myotube stages being compared. Dystrophin expression is detectable after myoblast fusion and shows a predominantly sarcolemmal distribution within a few days of myotube formation (*12–14*). We therefore compared $[Ca^{2+}]_i$ in normal versus dystrophic myotubes from human and mouse 6 to 15 days after myoblast fusion. Resting $[Ca^{2+}]_i$ values for normal mouse and human myotubes were 82 ± 7 nM (mean ± SEM) (n = 45) and 55 ± 5 nM (n = 78), respectively (Fig. 1); the analogous values for myotubes from the *mdx* mouse and Duchenne human were already significantly elevated [110 ± 7 nM (n = 64) and 76 ± 5 nM (n = 78), respectively]. Exposure to a tenfold increase in extracellular Ca^{2+} (18 mM) showed $[Ca^{2+}]_i$ in normal mouse myotubes to be tightly regulated, whereas $[Ca^{2+}]_i$ rose dramatically in *mdx* myotubes (Fig. 1A). Unlike $[Ca^{2+}]_i$ in normal mouse myotubes, $[Ca^{2+}]_i$ in normal human myotubes increased under these conditions. However, the rate of increase of $[Ca^{2+}]_i$ was significantly higher in the Duchenne human myotubes (Fig. 1B). Thus, the ability to regulate free $[Ca^{2+}]_i$ was impaired in myo-

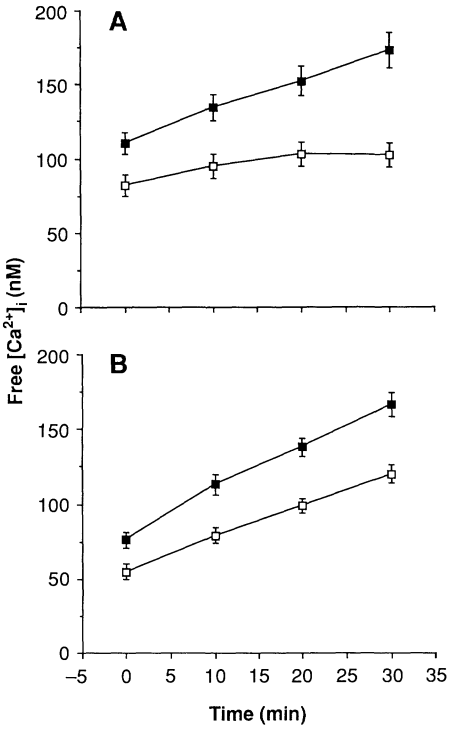

Fig. 1. Intracellular free Ca^{2+} estimated by fura 2 fluorescence in normal and dystrophic myotubes after a tenfold extracellular Ca^{2+} increase. (**A**) Normal mouse (□) and *mdx* mouse (■) myotubes and (**B**) normal human (□) and Duchenne human (■) myotubes. From 6 to 15 days after myoblast fusion, ratio images of myotubes were recorded over a 30-min period at the indicated time points (±1.5 min). At time 0, myotubes were bathed in a Ringer solution containing 1.8 mM extracellular Ca^{2+} (138 mM NaCl, 2.7 mM KCl, 1.8 mM $CaCl_2$, 1.06 mM $MgCl_2$, 12.4 mM Hepes, and 5.6 mM glucose, pH 7.2). Myotubes were then exposed to a Ringer solution containing 18.0 mM calcium. The mean $[Ca^{2+}]_i$ (nM ± SEM) is shown. Free Ca^{2+} was calculated as described (*21*).

Department of Molecular and Cell Biology, Division of Cell and Developmental Biology, University of California, Berkeley, CA 94720.

*To whom correspondence should be addressed.

tubes of dystrophic origin.

Calcium-selective leak channels, which are active at resting membrane potentials, may constitute a major pathway by which Ca^{2+} can enter myotubes (*15–18*). To test this possibility, we used patch techniques to record Ca^{2+} leak currents (*19*). In the cell-attached recording configuration, inward Ba^{2+} currents (Fig. 2) were observed at resting and hyperpolarized membrane potentials in myotubes bathed in a low-Ca^{2+} (0.18 mM) Ringer solution. Leak channel activity was present in ~50% of seals recorded for both normal and dystrophic myotubes from human and mouse (Fig. 2). This activity occurred in bursts (Fig. 2), a finding consistent with previous observations in cardiac ventricular myocytes (*18*). Because the channel activity persisted in inside-out patches, we conclude that adenosine triphosphate (ATP)–activated Ca^{2+} channels were not the source of the currents measured (*15*). Single-channel conductances, determined from current-voltage plots of the data, were about 10 pS (Fig. 3). As expected for Ba^{2+} currents under these recording conditions, the extrapolated reversal potentials were always positive. Identical results were obtained when we used the physiologically relevant divalent cation, Ca^{2+}, as the charge carrier. We also measured these currents with standard low-Ca^{2+} Ringer in the pipette, and the currents were unchanged when the Na^+ was reduced to 70 or 10 mM by the equimolar substitution with *N*-methyl-D-glucamine. These channel characteristics, which were identical in normal and dystrophic myotubes from human and mouse, closely resembled those of other Ca^{2+} leak or Ca^{2+} background channels (*15–18*).

We found that, although the mean leak channel open times were roughly similar in normal and dystrophic preparations (Fig. 4A), the mean closed times for channels from Duchenne and *mdx* myotubes were significantly shorter than normal values (Fig. 4B). Channel closed times from dystrophic myotubes were about one-third of those from normal myotubes. The calculated open probability (P_o) was 0.028 in normal human leak channels and 0.085 in Duchenne human leak channels. The P_o was 0.008 in normal mouse and 0.020 in *mdx* mouse (Fig. 5, A to D). Such a 2.5- to 3-fold increase in channel P_o could account for the increased basal free $[Ca^{2+}]_i$ in dystrophic myotubes. No voltage-dependent variation in closed times was seen for this channel type. The difference in P_o between normal and dystrophic channels is unlikely to be the result of cytoplasmic factors, as

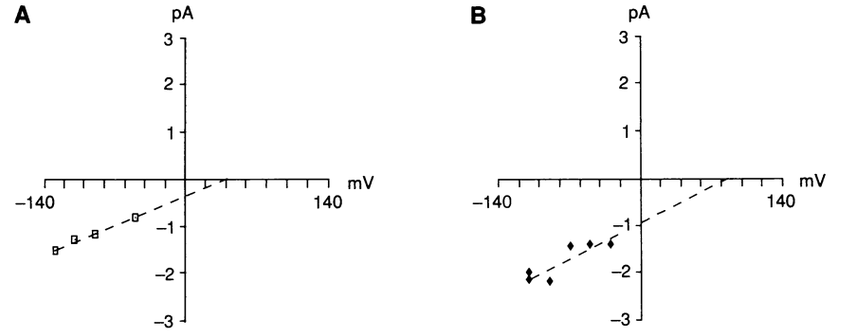

Fig. 3. Current-voltage relations for Ca^{2+} leak channels in excised patches from (**A**) Duchenne human and (**B**) *mdx* mouse myotubes. A least-square fit of the data was performed (dotted lines). The average reversal potential was +43 ± 4.7 mV, and slope conductance was 9.87 ± 0.59 pS in eight excised patches of human and mouse origin. Channels recorded in the cell-attached configuration exhibited the same properties (22 patches). Upon formation of an on-cell seal, the membrane potential was gradually hyperpolarized in 20-mV increments and held at these steady-state levels until channel activity was observed and recorded. Patches were excised at a holding potential of −50 mV, and the protocol was repeated.

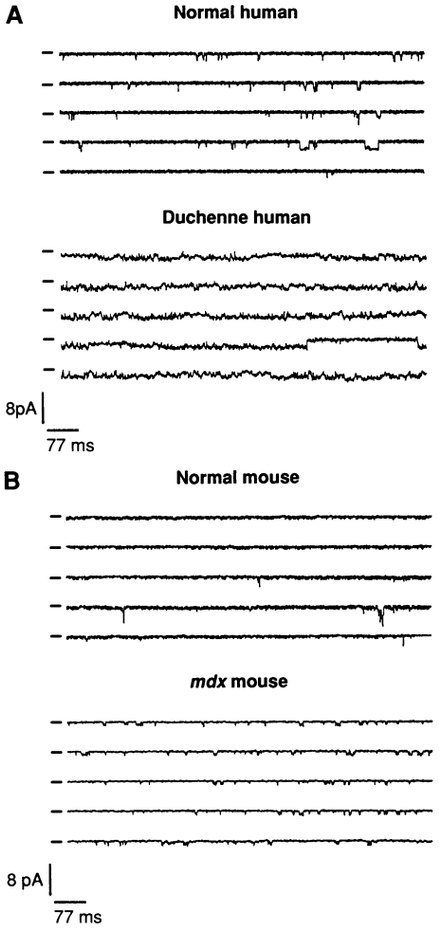

Fig. 2. Representative recordings of episodic Ca^{2+} leak channel activity made in (**A**) normal and Duchenne human and (**B**) normal and *mdx* mouse myotubes. The normal mouse record shows multiconductance states seen occasionally in both normal and *mdx* myotubes. Records are from cell-attached patches, with Ba^{2+} as the charge-carrying species. Holding potentials (110 mV) were calculated with an estimated resting potential of −50 mV. Inward current is depicted as a downward deflection of the trace. Recordings were filtered at 2000 Hz (−3 dB, four-pole Bessel low-pass filter), then filtered again on playback at a frequency of 500 Hz. Myotubes were in a low-Ca^{2+} Ringer solution (140 mM NaCl, 2.7 mM KCl, 0.8 mM $CaCl_2$, 1.06 mM $MgCl_2$, 12.4 mM Hepes, and 5.6 mM glucose, pH 7.2) for recording, to minimize the chance of spontaneous contractions. Patch pipettes were fire-polished to resistances of 5 to 13 megohms and filled with 96 mM $BaCl_2$, 12.4 mM Hepes, pH 7.2. All solutions were passed through 0.22-μM filters (Gelman Scientific, Ann Arbor, Michigan). Data were acquired with an Axopatch 1-C patch clamp amplifier (Axon Instruments, Foster City, California). Seals were formed by the release of positive pressure, and resistances ranged from 1 to 30 gigohms. After cell-attached recording, patches were excised. Experiments were at 24°C.

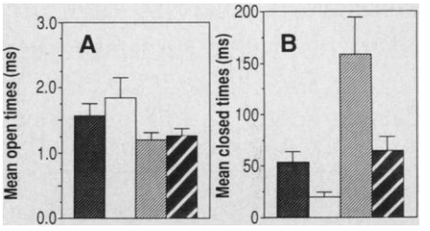

Fig. 4. (**A**) Mean open times for Ca^{2+} leak channels from normal (black bars) and Duchenne (white bars) human myotubes, and normal (gray bars) and *mdx* (striped bars) mouse myotubes. Data were analyzed by computer (pClamp; Axon Instruments). Mean open times (± SEM) were 1.6 ± 0.19 ms in data from 8 normal human patches, and 1.8 ± 0.31 ms from 6 Duchenne human patches ($P > 0.10$, not significant); and 1.2 ± 0.11 ms in 18 normal mouse patches and 1.3 ± 0.10 ms in 23 *mdx* mouse patches ($P > 0.10$, not significant). (**B**) Mean leak channel closed times were 55.5 ± 10.28 ms in 6 normal human patches, and 19.4 ± 4.96 ms in 8 Duchenne human patches ($P < 0.001$, highly significant); 158.4 ± 35.7 ms in 15 normal mouse patches and 64.4 ± 13.77 ms in 19 *mdx* mouse patches ($P < 0.01$, highly significant). Closed and open time distributions have been fitted, and time constants calculated as described (*22*).

open and closed times in inside-out excised patches were similar to those in the cell-attached patches from which they were derived. In addition, under our recording conditions of 0.18 mM extracellular Ca^{2+}, cytoplasmic $[Ca^{2+}]_i$ measured in dystrophic preparations was not significantly different from normal (*1*).

The absolute closed time values appeared to be related to the ability to regulate $[Ca^{2+}]_i$. Normal mice, which showed the least Ca^{2+} leak channel activity (Fig. 4B), were best able to tightly regulate $[Ca^{2+}]_i$ levels after exposure to increased levels of extracellular Ca^{2+} (Fig. 1A). Normal human and *mdx* mouse myotubes, which had similar higher levels of Ca^{2+} leak channel activity, were less able to regulate $[Ca^{2+}]_i$ in response to a tenfold increase in extracellular Ca^{2+} (Fig. 1). The Duchenne human Ca^{2+} leak channels were by far the most active and these myotubes were the least able to regulate $[Ca^{2+}]_i$, as judged by the rate of increase in $[Ca^{2+}]_i$ when challenged with high Ca^{2+}. This may explain in part why muscle necrosis in Duchenne humans is usually eventually fatal, whereas the *mdx* mouse rebounds from the initial degenerative insult.

We tested modulators of voltage-gated and leak Ca^{2+} channels. Cadmium (0.5 mM), Co^{2+} (2 mM), Bay K 8644 (10 μM), and nifedipine (10 μM) were each added to the pipette solutions before patch formation and subsequent excision. At these concentrations, neither Cd^{2+} nor Co^{2+} significantly altered Ca^{2+} leak channel activity in either normal or *mdx* mouse myotubes. It has been reported that these inorganic ions, which block voltage-gated Ca^{2+} channels, have no effect on the rat ventricular myocyte Ca^{2+} leak channels, whereas the 1,4-dihydropyridine (DHP) analogs Bay K 8644 and nitrendipine enhance channel activity (*18*). In our experiments, both the DHP agonist, Bay K 8644, and the DHP antagonist, nifedipine, increased channel activity in normal mouse myotube leak channels, demonstrating that the myotube leak channel has pharmacological properties similar to those of the Ca^{2+} leak channel described in ventricular myocytes (*18*). Since nifedipine could act as an agonist for these Ca^{2+} leak channels, we tested its effect on $[Ca^{2+}]_i$. Nifedipine (10 μM), which increased P_o 1.7-fold in normal mouse myotubes, also increased $[Ca^{2+}]_i$ as expected in myotubes, from a resting value of 119 ± 3 nM to 144 ± 5 nM (n = 4), a highly significant difference ($P < 0.001$). Single fibers from normal adult flexor digitorum brevis muscle responded in similar fashion to nifedipine; 10 μM nifedipine increased $[Ca^{2+}]_i$ from 124 ± 3 nM to 137 ± 2 nM (n = 3) ($P < 0.01$). These results support our interpretation that the Ca^{2+} leak channels described here are influencing the levels of $[Ca^{2+}]_i$ in both myotubes and adult muscle. A recent report has described stretch-inactivated channels that are more abundant in *mdx* mouse myotubes and that could also contribute to higher levels of $[Ca^{2+}]_i$ (*20*).

In conclusion, the results presented here suggest that an increase in Ca^{2+} leak channel activity in myotubes of both *mdx* mouse and Duchenne human origin could contribute to the observed elevation of $[Ca^{2+}]_i$. These findings, and our previous demonstration of a relation between $[Ca^{2+}]_i$ and protein degradation rates in dystrophic muscle (*1*), suggest that increased Ca^{2+} entry through Ca^{2+} leak channels may lead to the pathology of dystrophic muscle.

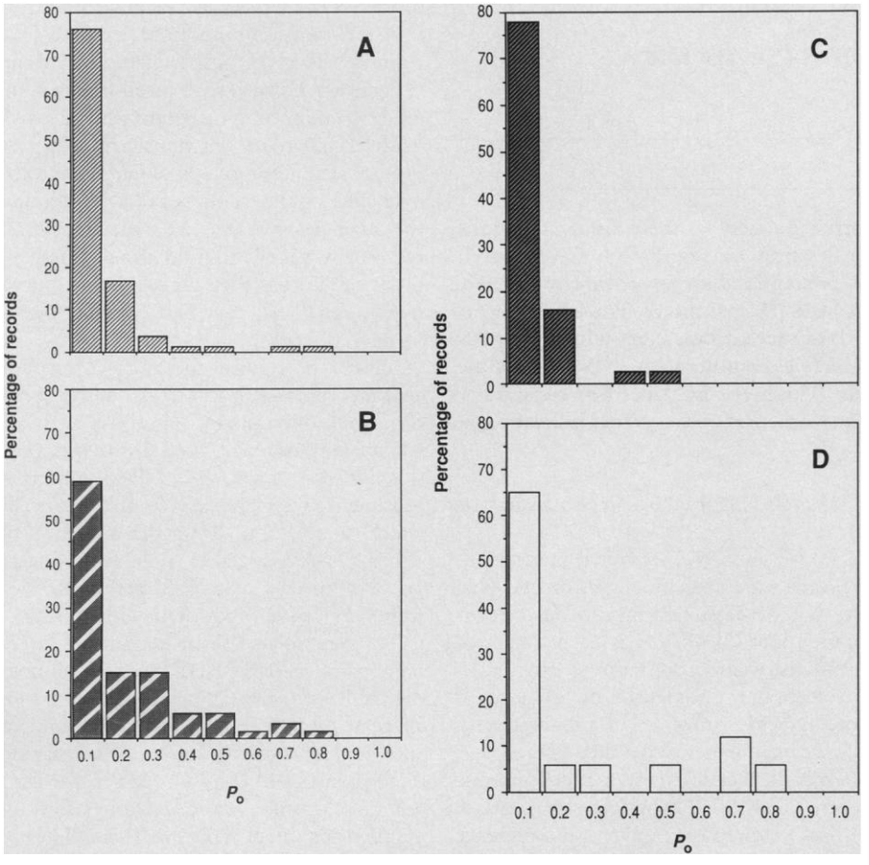

Fig. 5. Channel P_o values were calculated using the relationship (mean open time)/(mean open time + mean closed time). The increase in P_o occurred over the entire range of channel activity. The average P_o values were (**A**) for normal mouse, 0.008; (**B**) for *mdx* mouse, 0.020; (**C**) for normal human, 0.028; and (**D**) for Duchenne human, 0.085.

REFERENCES AND NOTES

1. P. R. Turner, T. Westwood, C. R. Regen, R. A. Steinhardt, *Nature* **335**, 735 (1988).
2. E. P. Hoffman, R. H. Brown, Jr., L. M. Kunkel, *Cell* **51**, 919 (1987).
3. E. P. Hoffman, C. M. Kudson, K. P. Campbell, L. M. Kunkel, *Nature* **330**, 754 (1987).
4. J. S. Chamberlain *et al.*, *Science* **239**, 1416 (1988).
5. H. Sugita *et al.*, *Proc. Jpn. Acad.* **64B**, 37 (1988).
6. E. E. Zubryzcka-Gaarn *et al.*, *Nature* **333**, 466 (1988).
7. M. D. Baron, M. D. Davison, P. Jones, D. R. Critchley, *J. Biol. Chem.* **262**, 2558 (1987).
8. M. D. Davison and D. R. Critchley, *Cell* **52**, 159 (1988).
9. K. P. Campbell and S. D. Kahl, *Nature* **338**, 259 (1989).
10. J. M. Ervasti *et al.*, *ibid.* **345**, 315 (1990).
11. T. Mongini *et al.*, *Neurology* **38**, 476 (1988).
12. A. A. Lev, C. C. Feener, L. M. Kunkel, R. H. Brown, Jr., *J. Biol. Chem.* **262**, 15817 (1987).
13. U. Nudel, K. Robzyk, D. Yaffe, *Nature* **331**, 177 (1988).
14. A. F. Miranda *et al.*, *Am. J. Pathol.* **132**, 410 (1988).
15. C. D. Benham and R. W. Tsien, *Soc. Gen. Physiol. Ser.* **42**, 45 (1987).
16. M. D. Coyne, D. Dagan, I. B. Levitan, *J. Membr. Biol.* **97**, 205 (1987).
17. R. L. Rosenberg, P. Hess, R. W. Tsien, *J. Gen. Physiol.* **92**, 27 (1988).
18. A. Coulombe, I. A. Lefevre, I. Baro, E. Coraboeuf, *J. Membr. Biol.* **111**, 57 (1989).
19. O. P. Hamill, A. Marty, E. Neher, B. Sakmann, F. J. Sigworth, *Pfluegers Arch.* **391**, 85 (1981).
20. After our manuscript was first submitted, an interesting study of stretch-gated channels in mouse myotubes appeared [A. Franco, Jr., and J. B. Lansman, *Nature* **344**, 670 (1990)]. The chief similarity of this study to our work is their report of increased numbers of very active channels in *mdx* mouse myotubes which could carry a Ba^{2+} or Ca^{2+} current at high inside negative potentials. Their active channels in *mdx* myotubes were inactivated by stretch. We found that stretch could affect activity in some channels. However, very active channels in *mdx*

myotubes often were not affected by stretch. To test directly the hypothesis that stretch will inactivate the active channels in *mdx* mouse, we stretched and measured $[Ca^{2+}]_i$ in individual fibers from the flexor digitorum brevis muscle from normal and *mdx* mice. Stretch increased $[Ca^{2+}]_i$ slightly in normal fibers and decreased $[Ca^{2+}]_i$ slightly in *mdx* fibers. However, a substantial difference remains. $[Ca^{2+}]_i$ at different sarcomere lengths was measured with fura 2 loaded as the acetomethoxy ester. Normal muscle had 133 ± 4 nM $[Ca^{2+}]_i$ in the relaxed state, and $[Ca^{2+}]_i$ in the same fibers increased slightly to 146 ± 3 when stretched (n = 14); *mdx* fibers had 174 ± 5 nM $[Ca^{2+}]_i$ when relaxed, and this value in the same fibers decreased slightly to 165 ± 1 nM when the fibers were stretched (n = 13). Normal relaxed sarcomere length was 2.20 ± 0.13 μm; normal stretched length was 3.04 ± 0.08 μm; *mdx* relaxed length was 2.12 ± 0.10 μm and *mdx* stretched length was 3.15 ± 0.11 μm.

21. Free Ca^{2+} was calculated from the fluorescence ratio obtained by dividing the fluorescence (500 to 530 nm) values from excitation at 350 nm by those at 385 nm [G. Grynkiewicz, M. Poenie, R. Y. Tsien, *J. Biol. Chem.* **260** (no. 6), 3440 (1985)]. It was necessary to correct the ratios obtained in calibration solutions because of increased dye fluorescence inside the myotubes at 385-nm excitation, resulting from differences in intracellular viscosity, ionic strength, or dye binding [(*1*); R. Y. Tsien and M. Poenie, *Cell Calcium* **6**, 145 (1985)]. A correction factor of 0.70 was determined by permeabilizing myotubes with 2500 units of *Staphylococcus aureus* alpha toxin (Gibco-BRL) per milliliter in Ringer solutions containing concentrations of free Ca^{2+} in the 60- to 600-nM range. Primary myoblasts were obtained from mouse hindlimb muscle as previously described [J. Dimario and R. C. Strohman, *Differentiation* **39**, 42 (1988)]. Normal human and Duchenne clonal myoblasts were from frozen stocks. Myoblast fusion was induced by culturing in Dulbecco's modified Eagles medium (DMEM) with 10% horse serum. In mouse and human cultures, myotubes were present 2 and 4 days after differentiation, respectively. Cultures were loaded with dye by exposure to 10 μM fura 2-AM (Molecular Probes, Eugene, OR) for 60 min at 25°C in DMEM under 5% CO_2/95% air. Measurements were at 37°C in the Hepes-buffered Ringer.

22. The normal human leak channel closed-time distribution could be fitted with three exponentials with time constant (τ) values of 0.678, 6.68, 11.42 ms. The analogous values for Duchenne channels were 0.335, 1.86, and 3.13 ms. Thus, although the number of closed states appears to be unaffected, the time constants are dramatically altered. In a similar fashion, the normal mouse leak channels closed-time distribution could be fitted with τ values of 0.646, 4.869, and 8.019 ms; the *mdx* τ values were 0.368, 2.199, and 3.381 ms. Open channel time distributions could be fitted with two exponentials and did not differ greatly with the dystrophic condition. Normal human open τ values were 0.433 and 2.04 ms. Normal mouse open τ values were 0.314 and 1.919 ms.

23. We thank W. G. Owen for critical reading of the manuscript and T. Heiman-Patterson and R. Ham for supplying clonal myoblasts from normal human and Duchenne patients. Supported by the NIH Institute of General Medical Sciences, the Muscular Dystrophy Association, and a generous gift from W. T. Baker.

18 April 1990; accepted 11 July 1990

An Unusual Form of Lipid Linkage to the CD45 Peptide

AKIKO TAKEDA* AND ABBY L. MAIZEL

Some protein kinases and phosphatases are myristoylated on their amino terminus, which perhaps contributes to subcellular localization or regulation. Glycoprotein CD45, a hematopoietic tyrosine phosphatase, was examined for fatty acid content. The CD45 protein incorporated [^{3}H]myristate, but little [^{3}H]palmitate. The label was not metabolized and reincorporated into amino acids or saccharides, as revealed by peptide maps of CD45 labeled with [^{3}H]myristate, ^{14}C-labeled amino acids, [^{35}S]methionine, or ^{125}I, and glycosidase treatments, respectively. The myristate label was resistant to mild alkaline methanolysis and was found in fatty acid and sphingosine, indicating an unusual form of lipid attachment to CD45.

CD45 [ALSO DESIGNATED T200, B220, Ly5, and the leukocyte common antigen (LCA)] is a transmembrane glycoprotein of most hematopoietic cells (*1*). Several isotypes of CD45 may be variably expressed in a lineage- and developmental stage–specific manner as a result of differential usage of extracellular, NH_2-side exons (*2*). The intracellular portion contains phosphorylated serine residues (*3*) and tyrosine phosphatase activity (*4*) that, in turn, activates T cell tyrosine kinase p56^{lck} (*5*). CD45 is also involved in signal transduction (*6*).

Because some NH_2-terminal myristoylated proteins are protein kinases or phosphatases (*7*), we examined myristic acid incorporation into CD45. It has been suggested that myristoylation exerted regulatory roles by directing the juxtaposition of acylated proteins with other cellular components such as membranes and other peptides. A Moloney leukemia virus–induced murine (A/Sn), CD4$^+$8$^-$ T lymphoma line, YAC-1 (*8*), was cultured overnight in the presence of [^{35}S]methionine, [^{3}H]myristic acid, or [^{3}H]palmitic acid, and the cell lysates were immunoprecipitated with monoclonal antibodies (MAbs) to an invariable segment of CD45 (*1*), the transferrin receptor, or actin, and then analyzed by one-dimensional SDS–polyacrylamide gel electrophoresis (SDS-PAGE) (*9*) (Fig. 1A). The incorporation of the myristic acid label into CD45 was comparable to the incorporation into the transferrin receptor and actin, a representative fatty acylated protein (*10*) and an *N*-acetylated protein (*11*), respectively. The incorporation of palmitic acid into the transferrin receptor was as efficient as that of myristic acid. In contrast, palmitic acid was poorly incorporated into CD45 and actin. When a duplicate gel was treated with mild alkaline methanol (Fig. 1B), the fatty acid label incorporated into the transferrin receptor disappeared almost completely, while the treatment only slightly affected the label incorporated into CD45 and actin. Alkaline methanolysis releases fatty acyl groups from thio- as well as hydroxy-ester linkages without affecting peptide bonds (*12*); accordingly, the treatment did not alter the methionine label for any of the molecules examined (*13*).

The incorporation of the fatty acid label into actin was probably due to degradation of fatty acid into the acetyl form, which could be amide-linked to the NH_2-terminus of actin. The myristic acid label incorporated into the transferrin receptor may be in a palmitoyl form because of fatty acid chain elongation. However, in a cell-free system, either palmitate or myristate can be covalently attached to the transferrin receptor (*14*). A significant degree of fatty acid turnover into amino acids is unlikely, because the label incorporated into the transferrin receptor was labile to mild alkaline methanolysis, indicating that the label was indeed incorporated as the fatty acyl–thioester form.

In order to confirm that the [^{3}H]myristic acid incorporated into CD45 had not been converted into amino acids, we analyzed tryptic peptides of CD45 by two-dimensional (2-D) "mapping." CD45 immunoprecipitates were prepared from YAC-1 cells which were cultured in the presence of either [^{3}H]myristic acid, a ^{14}C-labeled amino acid mixture, or [^{35}S]methionine, or were surface-radioiodinated with ^{125}I (*15*). CD45 was isolated from excised gel pieces of preparative SDS-PAGE by electroelution, digested with trypsin overnight, and subjected to electrophoresis in the first dimension and chromatography in the second dimension (*3, 16*) (Fig. 2). Clearly, the fatty acid label was not incorporated in a form of amino acids, because in that event ^{3}H- and ^{14}C-labeled peptides should have shared a similar distribution pattern. Instead, virtually all ^{3}H-labeled peptides were found along the electrophoresis axis, whereas only ap-

Department of Pathology, Roger Williams General Hospital, Brown University, Providence, RI 02908.

*To whom correspondence should be addressed.